

### General comments

The paper describes a case study of concentric gravity waves (CGWs) observed with the airglow imager in Brazil on 17-18 September 2023. Also, these CGWs were simultaneously captured by three satellites. Three groups of intense CGWs lasted over 10 hours. The CGWs caused profound airglow emission perturbations exceeding 24%. These CGW events were caused by fast-moving deep convections observed by the GOES-16 satellite. The authors have found that these CGW events represent the most intense vertical transport cases ever recorded, demonstrating remarkable wave coupling between the lower and upper atmosphere. I have found the paper to be interesting to the atmospheric community. At the same time, I have found a number of issues that should be explained in more detail. That is why I recommend accepting the paper after major revision.

We sincerely appreciate your thoughtful and constructive feedback on our manuscript. We are grateful for the time and effort dedicated to evaluating our work, especially the recognition of its significance to the atmospheric community. Your insightful comments have helped us identify areas where the study can be further strengthened. The detailed technical comments have helped us significantly improve the rigor and clarity of the study. Below, we address each point in detail and have incorporated substantial revisions to improve clarity, methodology, and discussion as suggested.

### Specific comments

Line 71: "...dual-layer airglow observations..." It is not clear what dual-layer the authors talk about? It should be clarified here.

Reply: Thank you very much for your comment. We have provided the following clarification regarding dual-layer airglow observations:

"Although the observation of AGWs by airglow imagers has been widely documented in previous studies (Dalin et al., 2024; Nyassor et al., 2021, 2022; Suzuki et al., 2007a; Vadas et al., 2012; Vargas et al., 2021; Wüst et al., 2019; Xu et al., 2015; Yue et al., 2009), dual-layer airglow observations, which involve observing airglow emissions from a hydroxyl radical (OH) layer (~87 km) in the mesosphere and an atomic oxygen emission layer at 630 nm (OI 630.0 nm) (~250 km) in the thermosphere, offer a unique opportunity to simultaneously investigate CGWs in both the mesosphere and thermosphere. This configuration enables comprehensive studies of gravity wave vertical propagation and their role in vertical atmospheric coupling. However, due to past limitations in observational capabilities, simultaneous detection of CGWs across both the OH and OI 630.0 nm layers was rare."

Line 76: "... across these two atmospheric layers was rare." Across which two layers?

Reply: The two layers are OH and OI 630.0 nm layers, respectively.

Lines 86-87: "...São Martinho da Serra..." Please add Brazil here.

Reply: Thank you. The revision has been made as requested.

Lines 93-95: "The time resolution of the OH airglow image is 112 seconds, while that of the OI 630 nm airglow image is 225 seconds." Is it the time resolution or exposure time? What is the exposure time?

Reply: The time mentioned is the temporal resolution of airglow images. The exposure times of the OH airglow image and the OI 630 nm airglow image are 20 s and 90 s, respectively.

Line 98: "...the effective observation ranges of OH airglow imager with a 164° field of view" Before it was said that "fish-eye lens of a 180° field of view" What is true?

Reply: We appreciate your careful attention to the field of view (FOV) details. The fisheye lens itself has a 180° FOV. However, as you noted, we intentionally selected a 164° FOV as the effective observation range for our analysis. This is because the image distortion and stretching become increasingly severe near the edges of the fisheye lens, which would compromise the accuracy of our airglow measurements.

Lines 101-102: "Before effectively extracting the wave parameters, the raw airglow images need to be processed through the following steps:..." It is not a complete information on the processing of raw images. Among others, the following steps should be described: How the atmospheric background was subtracted? How the dark noise of the sensor was subtracted? How the flat field correction (non-uniformity of the sensor at different wavelengths) was taken into account? Was the imager absolutely calibrated in a lab? Does the imager register airglow intensities in relative or absolute units (Rayleigh)? At which solar depression angles does the imager operate?

Reply: My sincere apologies for not providing a detailed description of the process, which may have caused you confusion. We have provided the detailed process as follows:

"Before effectively extracting the wave parameters, the raw airglow images need to be processed through the following steps: First, a median filter with a kernel size of  $17 \times 17$  pixels was employed to eliminate stars from the raw images (Li et al., 2011). We also removed the CCD dark noise, which was estimated from dark-frame images captured with the shutter closed prior to observations. Second, we corrected for the van Rhijn effect and atmospheric extinction using the approach described in Kubota et al. (2001). The observed airglow intensity  $I(\theta)$  from the ground is not uniform across different zenith angles. This non-uniformity is due to the van Rhijn effect. Additionally, the observed airglow intensity is influenced by atmospheric extinction, which results

from absorption and scattering along the line of sight.

Since airglow observations are subject to the van Rhijn effect, the measured emission intensity at a specific zenith angle ( $\theta$ ) follows the relation (Kubota et al., 2001):

$$I(\theta) = I(0) \cdot V(H, \theta),$$

$$V(H, \theta) = \left[ 1 - \left( \frac{R}{R+H} \right)^2 \sin^2(\theta) \right]^{-1/2}, \quad (1)$$

where  $I(0)$  is the emission intensity at zenith.  $V(H, \theta)$  is the van Rhijn correction factor.  $R$  is the earth radius and  $H$  is the height of OH airglow layer. The relationship between the observed emission intensity  $I(\theta)$ —affected by atmospheric extinction—and the true emission intensity  $I_{true}(\theta)$  at the airglow layer is described by Kubota et al. (2001).

$$I(\theta) = I_{true}(\theta) \cdot 10^{-0.4 \cdot a \cdot F(\theta)},$$

$$F(\theta) = \left[ \cos \theta + 0.15 \cdot (93.885 - \theta \cdot \frac{180}{\pi})^{-1.253} \right]^{-1}, \quad (2)$$

where  $a$  is the atmospheric extinction coefficient,  $F(\theta)$  is an empirical equation.

Consequently, the image correction factor, obtained from the combination of Eqs. (1) and (2), takes the form:

$$K = V(H, \theta) \cdot 10^{-0.4 \cdot a \cdot F(\theta)}. \quad (3)$$

The parameter  $a$  depends on the atmospheric observing conditions. For the observed CGW events, we treat  $a$  as temporally constant. By averaging the images over the observation period, we derive the zenith-angle-dependent airglow intensity profile. The optimal value of  $a$  is determined by matching this observed profile with theoretical  $K$  profiles across varying  $a$ . The fitted value of parameter  $a$  is approximately 0.42. Finally, we apply the flat-field correction by dividing the raw images by the corresponding  $K$  factor.

Third, we eliminated atmospheric background counts from the images. For background emission, Swenson and Mende (1994) used simultaneous Infrared measurements to demonstrate that the background contributes approximately 30% of the total OH airglow image signal. Similarly, Suzuki et al. (2007b) confirmed this ratio (~30%) through concurrent OH intensity observations with a Spectral Airglow Temperature Imager. In this study, we adopt the same assumption that background emissions account for ~30% of the total signal.”

The imager was not absolutely calibrated in the lab. As a result, it only measures

airglow intensities in relative units, not in absolute units like Rayleigh. Airglow observations are conducted when the solar depression angle is less than  $-12^\circ$  .

Swenson, G., and Mende, S. B.: OH emission and gravity waves (including a breaking wave) in all-sky imagery from Bear Lake, UT, *Geophys. Res. Lett.*, 21, 2239–2242, <https://doi.org/10.1029/94GL02112>, 1994.

Suzuki, S., Shiokawa, K., Otsuka, Y., Ogawa, T., Kubota, M., Tsutsumi, M., Nakamura, T., and Fritts, D. C.: Gravity wave momentum flux in the upper mesosphere derived from OH airglow imaging measurements, *Earth Planets Space*, 59, 421–428, <https://doi.org/10.1186/BF03352703>, 2007b.

Line 117: “Third, the processed images were projected onto geographic coordinates,...” This information is not enough. It should be described in more detail how the optical model of the imager optical system was determined and calculated? What were the reference points in order to calculate free parameters of the optical model? Stars or lab reference points? What are the errors of projected pixels in the image center and at the edge of FoV? What is the spatial resolution of the imager in the imager center and at the edge of FoV?

Reply: We have provided a detailed description as follows:

“Then, the original airglow images were spatially calibrated using stars as reference points. Each pixel location (i, j) in the original image was first mapped to a position (f, g) in a standardized coordinate system. Subsequently, the point (f, g) was transformed into geographic coordinates (x, y) using azimuth (az) and elevation (el) angles.

The conversion between original image coordinates (i, j) and standard coordinates (f, g) is defined by a linear transformation (Hapgood and Taylor, 1982):

$$\begin{bmatrix} f \\ g \end{bmatrix} = \begin{bmatrix} a_0 & a_1 & a_2 \\ b_0 & b_1 & b_2 \end{bmatrix} \begin{bmatrix} 1 \\ i \\ j \end{bmatrix}, \quad (1)$$

where the coefficients a and b are calculated by applying a least-squares fitting using the observed location of the stars in the original image and their locations in standard coordinate (Garcia et al., 1997):

$$\begin{bmatrix} a_0 & b_0 \\ a_1 & b_1 \\ a_2 & b_2 \end{bmatrix} = \begin{bmatrix} \mathbf{1}^T \mathbf{1} & \mathbf{1}^T \mathbf{i} & \mathbf{1}^T \mathbf{j} \\ \mathbf{1}^T \mathbf{i} & \mathbf{i}^T \mathbf{i} & \mathbf{i}^T \mathbf{j} \\ \mathbf{1}^T \mathbf{j} & \mathbf{i}^T \mathbf{j} & \mathbf{j}^T \mathbf{j} \end{bmatrix}^{-1} \begin{bmatrix} \mathbf{1}^T \\ \mathbf{i}^T \\ \mathbf{j}^T \end{bmatrix} \begin{bmatrix} \mathbf{f} & \mathbf{g} \end{bmatrix}, \quad (2)$$

where the column vectors  $\mathbf{i}$  and  $\mathbf{j}$  contain observed star locations in the original image, while  $\mathbf{f}$  and  $\mathbf{g}$  hold their computed normalized coordinates. The vector  $\mathbf{1}$  is a constant-valued column vector with length matching these vectors.

Through a georeference procedure, the standard coordinate images were projected onto geographic coordinates, assuming peak emission heights of 87 km for the OH layer and 250 km for the OH 630.0 nm layer. The spatial resolution of the imager varies significantly with zenith angle. For the OH channel, it is 0.53 km/pixel at the center of the image and degrades to 39.8 km/pixel at the edge of the image. For the 630 channel, the resolution is 1.53 km/pixel at the center of the image and decreases to 40.8 km/pixel at the edge of the image.”

You're absolutely right. There are projection errors. Hapgood and Taylor (1982) pointed out that there is some uncertainty in the position of any airglow structure due to the error in measuring the elevation and azimuth of the stars. The error of the stars in elevation is 2', corresponding error in the range to the airglow is ~1 km at 10° elevation, increasing to ~2 km at 5° elevation. They also studied the uncertainty in the position of any airglow structure caused by atmospheric refraction and found that it is less than the uncertainty arising from the error in measuring elevation. The CGWs we observed were almost exclusively within the field of view above an elevation angle of 10°; thus, these errors are not considered in this study.

Garcia, F. J., Taylor, M. J., and Kelley, M. C.: Two-dimensional spectral analysis of mesospheric airglow image data, *Appl. Optics*, 36, 7374–7385, <https://doi.org/10.1364/AO.36.007374>, 1997.

Hapgood, M. and Taylor, M. J.: Analysis of airglow image data, *Ann. Geophys.*, 38, 805–813, 1982.

Lines 122-129. It should be given a reference on the GOES-16 satellite and addressed visible and infrared parameters.

Reply: Thank you for your comments. The revision has been made as requested.

“The Geostationary Operational Environmental Satellite-16 (GOES-16) (Schmit et al., 2005), launched in November 2016, is part of the GOES-R Series. The Advanced Baseline Imager (ABI) is the primary instrument on GOES-16, providing high-resolution imagery in 16 spectral bands, including 2 visible channels (0.47  $\mu\text{m}$  and 0.64  $\mu\text{m}$ ), 4 near-infrared channels (0.86  $\mu\text{m}$ , 1.37  $\mu\text{m}$ , 1.6  $\mu\text{m}$ , and 2.2  $\mu\text{m}$ ), and 10 infrared channels (3.9–13.3  $\mu\text{m}$ ), with a temporal resolution of 10 min and a spatial resolution of 0.5–2 km (Schmit et al., 2017). The brightness temperature (BT), derived from 10.3  $\mu\text{m}$  infrared images from channel 13, is used to study the convection activities during the CGW events.”

Schmit, T. J., Gunshor, M. M., Menzel, W. P., Gurka, J. J., Li, J., and Bachmeier, A. S.: Introducing the next-generation advanced baseline imager on GOES-R, *Bull. Am. Met. Soc.*, 86, 1079-1096, doi:10.1175/BAMS-86-8-1079, 2005.

Schmit, T. J., Griffith, P., Gunshor, M. M., Daniels, J. M., Goodman, S. J., and Lebai, W. J.: A Closer Look at the ABI on the GOES-R Series. *Bulletin of the American Meteorological Society*, 98(4), 681–698, <https://doi.org/10.1175/bams-d-15-00230.1>, 2017.

Lines 139-141: “In this study, the CO<sub>2</sub> radiance emission band with frequencies ranging between 2299.80 cm<sup>-1</sup> and 2422.85 cm<sup>-1</sup> is utilized to measure stratospheric air temperature perturbations.” It should be given a reference on the Aqua satellite and CO<sub>2</sub> emissions used in this paper.

Reply: Thank you very much for your suggestion. The following references were added to the text.

Parkinson, C. L.: Aqua: an Earth-Observing Satellite mission to examine water and other climate variables, *IEEE Transactions on Geoscience and Remote Sensing*, 41(2), 173-183, <https://doi.org/10.1109/TGRS.2002.808319>, 2003.

Rothman, L. S., Gordon, I. E., Babikov, Y., Barbe, A., Chris Benner, D., Bernath, P. F., Birk, M., Bizzocchi, L., Boudon, V., Brown, L. R., Campargue, A., Chance, K., Cohen, E. A., Coudert, L. H., Devi, V. M., Drouin, B. J., Fayt, A., Flaud, J.-M., Gamache, R. R., Harrison, J. J., Hartmann, J.-M., Hill, C., Hodges, J. T., Jacquemart, D., Jolly, A., Lamouroux, J., Le Roy, R. J., Li, G., Long, D. A., Lyulin, O. M., Mackie, C. J., Massie, S. T., Mikhailenko, S., Müller, H. S. P., Naumenko, O. V., Nikitin, A. V., Orphal, J., Perevalov, V., Perrin, A., Polovtseva, E. R., Richard, C., Smith, M. A. H., Starikova, E., Sung, K., Tashkun, S., Tennyson, J., Toon, G. C., Tyuterev, V. I., and Wagner, G.: The HITRAN2012 molecular spectroscopic database, *J. Quant. Spectrosc. Radiat. Transfer*, 130, 4–50, <http://dx.doi.org/10.1016/j.jqsrt.2013.07.002>, 2013.

Lines 143-144: “The Visible Infrared Imaging Radiometer Suite (VIIRS) instrument, onboard the Suomi NPP satellite...” It should be given a reference on the Suomi NPP satellite.

Reply: Thank you very much for your suggestion. The following references were added to the text.

Lee, T. F., Nelson, S.C., Dills, P., Riishojgaard, L.P., Jones, A., Li, L., Miller, S., Flynn, L.E., Jedlovec, G., McCarty, W., Hoffman, C., and McWilliams, G.: NPOESS: Next-generation operational global Earth observations, *Bull. Am. Meteorol. Soc.*, 91, 727–740, <https://doi.org/10.1175/2009BAMS2953.1>, 2010.

Lewis, J. M., Martin, D. W., Rabin, R. M. and Moosmüller, H.: Suomi: Pragmatic visionary, *Bull. Am. Meteorol. Soc.*, 91, 559–577, <https://doi.org/10.1175/2009BAMS2897.1>, 2010.

Lines 166-167: “CGW no. 1 first appeared in the southeast direction of the station.” Is it in the southeast or in the southwest direction of the station?

Reply: I'm sorry. I made a mistake. CGW no. 1 first appeared in the southwest direction of the station.

Lines 172-175: “...the center moved approximately 436 km westward, with an average speed reaching ~65 km/h. This eastward drift of the wave's center could be indicative of the influence of prevailing wind patterns and the westward movement of the convective system itself.” I hardly understand was it the eastward or westward drift? Or sometimes westward and sometimes eastward? This should be clarified.

Reply: I'm sorry. I made a mistake. The “westward” should be “eastward”. We have made the following revisions:

“...the center moved approximately 436 km eastward, with an average speed reaching ~65 km/h. This eastward drift of the wave's center could be indicative of the influence of prevailing wind patterns and the eastward movement of the convective system itself.”

Lines 173-174: “This eastward drift of the wave's center could be indicative of the influence of prevailing wind patterns...” This is very interesting but it is not entirely clear. At what altitude is the prevailing wind considered? In the tropopause or in the mesopause?

Reply: Thank you very much for your comments. The following description has been added to the main text.

“Apart from the moving convective system mentioned above, which is a primary cause of the eastward displacement of the CGW center observed at the mesopause, the prevailing winds near 10 km and 55 km in Fig. 9a also significantly contribute to the eastward movement of the CGW center.”

Lines 176-177: “...are measured to be  $(30-82) \pm 3$  km.” Having such a large range of wavelengths what is the physical sense of indicating the error of 3 km? What does this error tell us? Is it the instrumental error or geophysical wave variability or both? This is again connected to my above-mentioned questions on What are the errors of projected pixels in the image center and at the edge of FoV?

Reply: I highly admire your rigorous comments.

I'd like to clarify that the 30–82 km range indicates radial variations of horizontal wavelengths, while the  $\pm 3$  km represents the variation of wavelengths along the circular arc direction.



In Figs. 2 and 3, what physical quantity can we see on these images? Is it some raw OH emission intensity? Or is it a corrected emission intensity? Or is it OH emission intensity in absolute values? It should be clarified in the figure captions.

Reply: Thank you very much for your comments. The following descriptions are added to captions of Figs. 2 and 3.

“The presented images display the corrected OH emission intensity.”

In Fig. 3, it is difficult to see the green and light blue dots and arrows for color-blind readers. I recommend changing the green dots to, for example, green triangles.

Reply: Following your suggestions, we have made revisions to Fig. 3, as shown below:

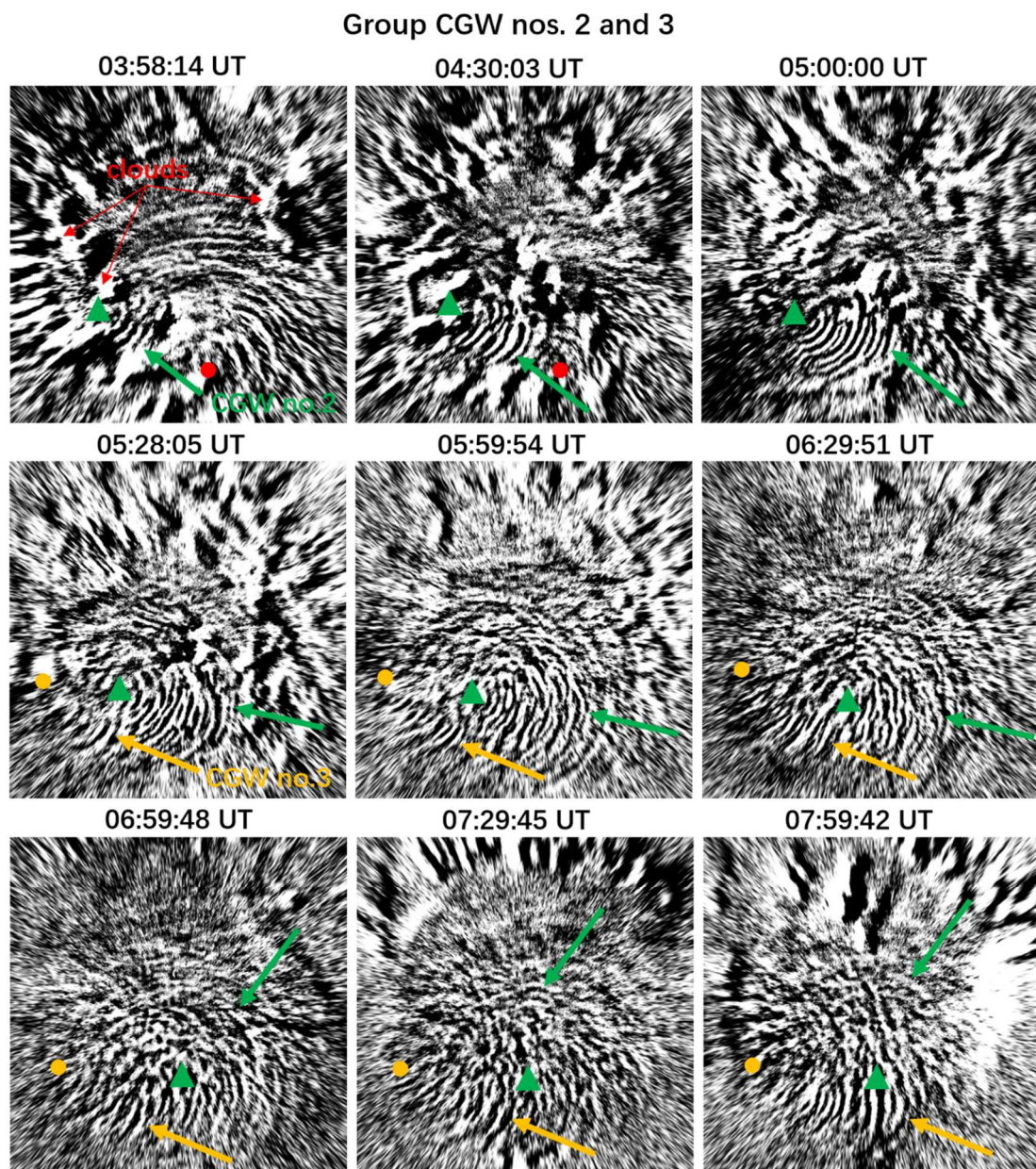




**Figure 3.** All-sky OH images projected onto an area of 1000 km × 1000 km showing the CGW no. 2 and CGW no. 3 events at half-hour intervals in the SMS station on 18 September 2023. The red dot marks the estimated center of the CGW no. 1, while the green triangles and orange yellow dots indicate the estimated centers of the CGW no. 2 and CGW no. 3, respectively. The presented images display the corrected OH emission intensity.

Caption to Fig.6, please indicate the approximate altitude at which this temperature map is observed.

Reply: We have made the following modifications to the caption of Fig. 6.

“Figure 6. Aqua satellite 4.3 μm brightness temperature observations of CGWs at 05:05:21 UT on 18 September 2023. Brightness temperature is derived from 4.3 μm radiance at an altitude range of 30–40 km. The red triangle and dot mark the SMS station and fitted wave center, respectively.”

Line 267: “...horizontal wavelengths are primarily distributed within the range of (38–52) ± 3 km” Having such a large range of wavelengths what is the physical sense of indicating the error of 3 km?

Reply: Thank you very much for your comments.

I’d like to clarify that the 38–52 km range indicates radial variations of horizontal wavelengths, while the ±3 km represents the variation of wavelengths along the circular arc direction.

Lines 301-307. The sentence is repeated twice, please remove the repeated part.

Reply: We have removed the repeated part.

Lines 306-307: “... when their phase velocities fall within the prohibited range.” What is the prohibited range? How much is it?

Reply: We have elaborated on “prohibited range” as follows:

The dispersion relationship of GWs (Hines, 1960) is given by

$$m^2 = \frac{N^2}{(c-u)^2} - k^2 - \frac{1}{4H^2}, \quad (1)$$

where  $m$  and  $k$  are vertical and horizontal wavenumbers, respectively;  $c$  is the horizontal observed phase speed of the GW;  $u$  is the background wind speed in the wave propagation direction;  $N$  is the Brunt-Väisälä frequency; and  $H$  is the scale height. According to Eq (1), if the GW propagation speed is close to or equal to the horizontal wind speed in the wave propagation, the vertical wave number  $m$  will

become infinite, which means that when encountering a critical layer, GWs will not be able to propagate upwards.

A blocking diagram is used to represent the velocity distribution, and the GWs in this distribution area cannot propagate to a specific height due to the critical layer filtering effect. The blocking diagram is generated by the following equation:

$$c \leq V_z \cos \varphi + V_m \sin \varphi, \quad (2)$$

here  $V_z$  and  $V_m$  are zonal and meridional wind speed, respectively.  $\varphi$  is the azimuth (anticlockwise from the east) of the horizontal propagation direction.

“Prohibited range” refers to a speed range, as indicated by the areas at different times in Fig. 9c. The boundaries of these areas represent the maximum amplitude. In Fig. 9c, the maximum amplitude of the prohibited range is shown to be approximately 44 m/s.

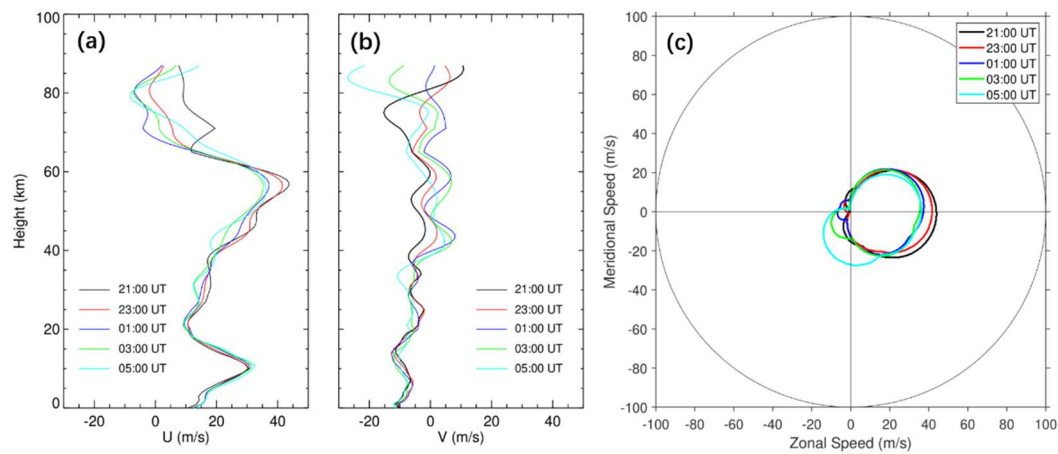


**Figure 9.** (a) The (a) zonal and (b) meridional wind field profiles from ERA5 (0-70 km) and HWM14 model (70-87 km) at 21:00 UT, 23:00 UT, 01:00 UT, 03:00 UT, and 05:00 UT, respectively. (c) Two-dimensional blocking diagrams from 0 to 87 km derived from the wind profiles in (a) and (b) on 17-18 September 2023.

Lines 322-327: “We also conducted a statistical analysis of CGWs observed by a meridional airglow observation network across mainland China from September 2023 to August 2024, with data from selected stations including Daicai (25.34°N, 110.34°E), Wendeng (37.18°N, 121.79°E), Mohe (53.48°N, 122.34°E), and Naqu (31.73°N, 92.47°E). The results indicate that the average CGW amplitudes ranged between 1.7% and 2.6%.” It seems to me that this is a completely different study, with completely different regions than the area of Brazil under discussion. A reference to this study is needed here. Otherwise it should be removed.

Reply: Thank you very much for your suggestion. We have removed the sentences you mentioned above.

Lines 332-334: “During the generation and propagation of CGWs, two saber orbits passed over the station and happened to be within the field of view of the airglow imager, as shown in Fig. 11.” How is the field of view of TIMED/SABER oriented in Fig.11? Please add this information.

Reply: Thank you very much for your comment. The field of view information has been added to the Fig.11 caption as shown below:

“Figure 11. Simultaneous observations of mesopause CGWs using OH channel ground-based all-sky airglow imager and TIMED/SABER satellite measurements. The red triangle marks the location of the SMS station. The instantaneous field of view of TIMED/SABER is 0.7 mrad by 10 mrad.”

Lines 341-342: “In addition to this, we also observed a double-peaked structure in the airglow emission layer.” Which airglow SABER profiles do demonstrate a double-peaked structure? This should be paid attention to.

Reply: Thank you for your comment. The following discussion has been added to the text.

“There are weak double-peak structures during the first overpass at 00:24:10 UT and 00:28:15 UT. In contrast, the double-peak structure is more prominent during the second overpass in the 07:18:23 UT profile.”

Lines 342-346: “From the temperature profiles (Fig. 12b and d), we have detected a rich spectrum of vertically propagating waves with vertical wavelengths between 5 km and 20 km, which consists with concurrent airglow and satellite observations of upward-propagating CGWs.” This sentence sounds very strange to me due to the following reasons: 1. There is no information at all about vertical spectrums of gravity waves derived from airglow and satellite observations. All presented data were about horizontal gravity wave patterns. Of course, using the dispersion relation for gravity waves one can derive a vertical wavelength from a horizontal wavelength, but it was not done in the manuscript so far. 2. Each presented temperature profile shows significant vertical variations, i.e., inside the FoV of the imager and outside it, far away from the imager. How can we be 100% sure that these temperature variations are due to CGWs and not other gravity waves? This sentence should be redeveloped or removed from the manuscript.

Reply: Thank you very much for your comments and suggestions, and we have removed the relevant description.

Equation 4. What is  $\omega$  here and how was it calculated? What is  $g$  here?

Reply: I'm really sorry for missing the information of these two parameters.

$\omega = \frac{2\pi c_i}{\lambda_h}$  is the intrinsic frequency (where  $c_i$  is the intrinsic phase speed),  $g$  is the gravitational acceleration.

Lines 365-366: "...u is the wind speed in the wave direction derived from meteor radar,..." I could not find any information on a meteor radar used in this study. This information should be provided. Is a meteor radar located in the proximity to the imager? What is the accuracy of estimation of the horizontal wind speed from meteor radar data in the wave direction discussed here?

Reply: I sincerely apologize for the mistake. Initially, we intended to utilize wind field data from meteor radar, but the location was too far from the station. As a result, we ultimately used wind field data from HWM14.

Equation 6. Where is  $\alpha$  in this equation? The authors do not provide information on how they estimated  $k$ ,  $m$ ,  $N$  parameters in relation to the vertical direction. I assume these parameters were calculated as mean values over the height range from the tropopause to the mesopause. But  $m$  and  $N$  may significantly vary with altitude, resulting in variations in the GW vertical group velocity (see for example, Fig. 4 in Dalin et al., 2016). This may provide significant deviation of the estimated propagation times. The author should provide a comment on Equation 6.

Reply: Thank you very much for your comments.

The definition of  $\alpha$  should be introduced after Eq. (7) in the text. The following comments have been added to the main text.

"The horizontal wavenumber  $k$  is derived from airglow images. The Brunt-Väisälä frequency  $N$  and vertical wavenumber  $m$  were calculated as the mean value over the atmospheric layer spanning from the tropopause to the mesopause. Notably, the background wind and temperature may exhibit significant altitudinal variations, resulting in substantial variations in the CGW vertical group velocity."

Lines 388-390: "The vertical group velocities of CGW no. 1, CGW no. 2, and CGW no. 3 are estimated to be 31–37 ms<sup>-1</sup>, 24–30 ms<sup>-1</sup>, and 26–29 ms<sup>-1</sup>, respectively." What is the source of these estimated ranges of the vertical group velocities? The uncertainty of which parameters affects the uncertainty in the estimation of the group velocities to a greater extent?

Reply: Thank you very much for your comments.

The estimated ranges of the vertical group velocities are derived from CGW parameter measurements in airglow images as well as background atmospheric temperature and

wind fields. We have re-estimated the vertical group velocities of CGW no. 1, CGW no. 2, and CGW no. 3. The background temperature for calculating the vertical group velocity of CGW no. 1, no. 2, and no. 3 was derived from TIMED/SABER profiles within effective FOV of the OH imager during the first orbit, the average of the first and second orbits, and the second orbit, respectively, while wind field data combined ERA5 (0–70 km) and HWM14 (70–87 km).

The vertical group velocities of CGW no. 1, CGW no. 2, and CGW no. 3 are re-estimated to be  $27\text{--}42\text{ ms}^{-1}$ ,  $21\text{--}32\text{ ms}^{-1}$ , and  $24\text{--}31\text{ ms}^{-1}$ , respectively.

For CGW no.1, the uncertainty in the group velocity estimation mainly comes from the wave parameters derived from airglow images. For CGW no.2 and CGW no.3, variations in background temperature and wind fields contribute more to the uncertainty in vertical group velocities.

Figure 14. What are the red dashed lines in Fig.14 a and b? And I assume that the red triangle marks the location of the SMS station. Right?

Reply: Thank you very much for your comments. We have made the following modifications to the caption of Fig. 14.

**“Figure 14.** (a) All-sky 630.0 nm imaging observation of thermospheric CGW (red dashed lines) at 01:41:57 UT on 18 September 2023. The yellow dot marks the estimated center of the thermospheric CGW. (b) All-sky OH imaging observation of mesospheric CGW at 00:54:48 UT on 18 September 2023. The red dashed lines mark out the mesospheric CGW with the same scale as the thermospheric CGW. The red dot marks the estimated center of the mesospheric CGW. (c) GOES-16 10.3  $\mu\text{m}$  brightness temperature at 00:20:20 UT on 17-18 September 2023. The red triangle marks the location of the SMS station. (d) Wind profiles from ERA-5 (0-70 km) and HWM14 (70-250 km) averaged between 01:00 UT and 02:00 UT on 18 September 2023.”

Lines 463-464: “...demonstrating their substantial impact on atmospheric dynamics and space weather.” Please provide more information on how these waves substantially impact on space weather.

Reply: Thank you very much for your suggestions. We provide more information on how these waves substantially impact on space weather as below:

“... demonstrating their substantial impact on atmospheric dynamics and space weather by (1) seeding traveling ionospheric disturbances (TIDs) that disrupt communications/GPS, (2) triggering plasma instabilities, and (3) altering thermospheric density, affecting satellite drag.”